ULTRA SONO GRAPHY

Prostate gland volume estimation: anteroposterior diameters measured on axial versus sagittal ultrasonography and magnetic resonance images

Seo Yeon Youn[1], Moon Hyung Choi[1,2], Young Joon Lee[1,2], Robert Grimm[3], Heinrich von Busch[3], Dongyeob Han[4], Yohan Son[4], Bin Lou[5], Ali Kamen[5]

[1]Department of Radiology, Seoul St. Mary's Hospital, College of Medicine, The Catholic University of Korea, Seoul, Korea; [2]Department of Radiology, Eunpyeong St. Mary's Hospital, College of Medicine, The Catholic University of Korea, Seoul, Korea; [3]Diagnostic Imaging, Siemens Healthcare, Erlangen, Germany; [4]Siemens Healthineers Ltd., Seoul, Korea; [5]Digital Technology and Innovation, Siemens Healthineers, Princeton, NJ, USA

Purpose: The aim of this study was to evaluate the accuracy of prostate volume estimates calculated from the ellipsoid formula using the anteroposterior (AP) diameter measured on axial and sagittal images obtained through ultrasonography (US) and magnetic resonance imaging (MRI).

Methods: This retrospective study included 456 patients with transrectal US and MRI from two university hospitals. Two radiologists independently measured the prostate gland diameters on US and MRI: AP diameters on axial and sagittal images, transverse, and longitudinal diameters on midsagittal images. The volume estimates, $volume_{ax}$ and $volume_{sag}$, were calculated from the ellipsoid formula by using the AP diameter on axial and sagittal images, respectively. The prostate volume extracted from MRI-based whole-gland segmentation was considered the gold standard. The intraclass correlation coefficient (ICC) was used to evaluate the inter-method agreement between $volume_{ax}$ and $volume_{sag}$, and agreement with the gold standard. The Wilcoxon signed-rank test was used to analyze the differences between the volume estimates and the gold standard.

Results: The prostate gland volume estimates showed excellent inter-method agreement, and excellent agreement with the gold standard (ICCs >0.9). Compared with the gold standard, the volume estimates were significantly larger on MRI and significantly smaller on US ($P<0.001$). The volume difference (segmented volume–volume estimate) was greater in patients with larger prostate glands, especially on US.

Conclusion: $Volume_{ax}$ and $volume_{sag}$ showed excellent inter-method agreement and excellent agreement with the gold standard on both US and MRI. However, prostate volume was overestimated on MRI and underestimated on US.

Keywords: Prostate gland volume; Magnetic resonance imaging; Ultrasonography; Interobserver variability; Inter-method variability

Key points: Prostate volume estimates as determined by the ellipsoid formula on ultrasonography (US) and magnetic resonance imaging (MRI) showed excellent correlations with the gold standard. The prostate volume estimates on MRI overestimated and those on US underestimated the volume. The volume difference was greater on US than on MRI for patients with larger prostate glands.

ORIGINAL ARTICLE

https://doi.org/10.14366/usg.22104
eISSN: 2288-5943
Ultrasonography 2023;42:154-164

Received: June 22, 2022
Revised: August 20, 2022
Accepted: October 24, 2022

Correspondence to:
Moon Hyung Choi, MD, PhD,
Department of Radiology, Eunpyeong St. Mary's Hospital, College of Medicine, The Catholic University of Korea, 1021 Tongil-ro, Eunpyeong-gu, Seoul 03312, Korea

Tel. +82-2-2030-3013
Fax. +82-2-2030-3026
E-mail: cmh@catholic.ac.kr

How to cite this article:
Youn SY, Choi MH, Lee YJ, Grimm R, von Busch H, Han D, et al. Prostate gland volume estimation: anteroposterior diameters measured on axial versus sagittal ultrasonography and magnetic resonance images. Ultrasonography. 2023 Jan;42(1):154-164.

Introduction

The incidence of prostate disease is high in adult men and increases with age [1]. The most frequent benign prostate disease is benign prostatic hyperplasia (BPH), and nearly one-third of all men experience symptomatic prostate enlargement [1,2]. BPH is common, affecting approximately 50% to 75% of men over the age of 50 years [3]. Prostate cancer is the second most common cancer and the fifth leading cause of cancer-related death among men in 2020 [4]. In patients with suspected symptoms of prostate disease, the primary examination is transrectal ultrasonography (US), with routine measurement of prostate volume [5]. Prostate volume is also important in patients with suspected prostate cancer and with an increase in prostate-specific antigen (PSA) levels, because the use of PSA density (PSAD), which is calculated as the PSA level divided by the prostate gland volume, can assist in the stratification of prostate cancer risk [6–8]. Conflicting results have been reported regarding the accuracy of US-based volume estimation: estimates using US have been reported in one study to underestimate and in another study to overestimate prostate gland volume [9,10].

Many studies have proven the usefulness of prebiopsy magnetic resonance imaging (MRI) to detect more clinically significant prostate cancer and less clinically insignificant cancer [11–14]. Therefore, prostate volume on MRI is also useful to stratify cancer risk by calculating the PSAD. The Prostate Imaging–Reporting and Data System (PIRADS) offers guidelines for obtaining, reviewing, and reporting prostate MRI. PIRADS recommends reporting prostate gland volume determined using manual or automated segmentation or calculated using an ellipsoid formulation based on three-axis diameters. PIRADS version 2.0 recommends measuring the anteroposterior (AP) diameter on axial images, although measurement using midsagittal images is recommended in PIRADS version 2.1 [15,16]. There is a theoretical risk of overestimating the AP diameter on axial images that are not perpendicular to the long axis of the prostate gland [17]. A previous study compared the accuracy of both methods on prostate MRI. This study showed that the PIRADS version 2.0 method was more accurate for measuring prostate gland volume compared with the segmented volume [18].

Regarding prostate volume measurement, it has not yet been established whether axial or sagittal images are better on prostate MRI. Considering the frequent use of transrectal US to evaluate the prostate gland, the same issue also seems important for US. Additionally, it is uncertain whether prostate volume estimates obtained using US can be directly compared with those derived from MRI. A previous study compared the differences in prostate volume estimates from US and MRI and those using the AP diameter on axial images and midsagittal images [9]. However, as the study included a small number of patients (n=21), further studies with more patients are needed. Moreover, inter-reader variability should be considered when using volume estimates measured by different observers as a reliable parameter for follow-up of the size of the prostate gland. The purpose of this study was to evaluate the accuracy of prostate volume estimates calculated from the ellipsoid formula using AP diameter measured on axial and sagittal images on US and MRI.

Materials and Methods

Compliance with Ethical Standards

This retrospective, multicenter study was approved by the institutional review boards of Seoul St. Mary's Hospital (KC21RISI0451) and Eunpyeong St. Mary's Hospital (PC21RASI0092). Informed consent for the patients was waived due to the retrospective study design.

Subjects

Patients who underwent prostate MRI examinations for clinically suspected prostate cancer between September 2018 and February 2020 in two university hospitals were eligible (n=1,576). In these hospitals, all transrectal US-guided prostate biopsies were performed by board-certified radiologists, while transrectal prostate US examinations in general were performed by physicians with varying levels of experience. Therefore, only patients who underwent transrectal US-guided biopsy were selected in order to guarantee a high image quality of the US examination. Among the eligible patients, the following were excluded: those who did not undergo transrectal US-guided biopsy within 1 month before and after MRI (n=1,064), as well as patients with MRI obtained at 1.5 T (n=55) or with severe artifacts on MRI (n=1). A total of 456 patients were included in this study (327 and 129 patients from each hospital) (Fig. 1). Clinical information on age, PSA level, biopsy results, and prostatectomy results (if available) was collected.

MRI Acquisition

Either biparametric MRI or multiparametric MRI was included in this study (88 biparametric MRI and 368 multiparametric MRI). Prostate MRI was performed using 3-T MRI (MAGNETOM Verio or MAGNETOM Vida, Siemens Healthcare, Erlangen, Germany) with a surface coil and a spine coil. Although three-plane T2-weighted images (T2WI), T1-weighted images, and diffusion-weighted images were included in all MRI examinations and dynamic contrast-enhanced MRI in multiparametric MRI, only true axial and sagittal T2WI were used in the present study. Detailed parameters of T2WI are summarized in Table 1.

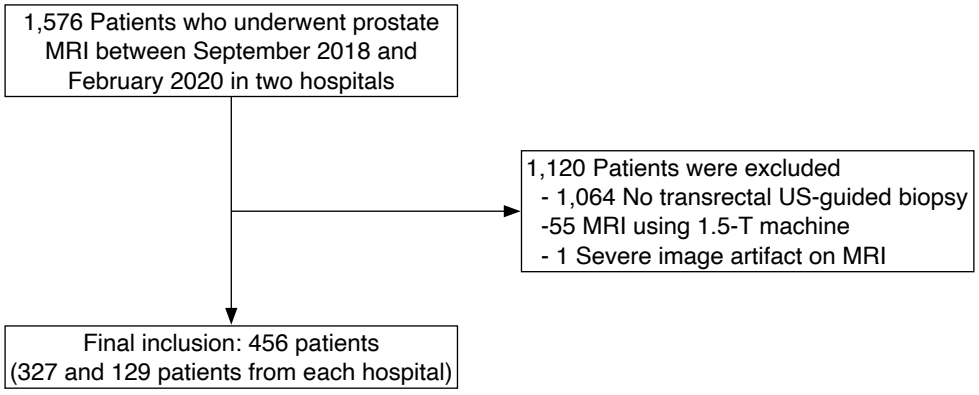

Fig. 1. Study patient inclusion flow chart. MRI, magnetic resonance imaging; US, ultrasonography.

Table 1. Parameters of T2WI

	Institution A				Institution B	
	MAGNETOM Vida		MAGNETOM Verio		MAGNETOM Vida	
	Axial	Sagittal	Axial	Sagittal	Axial	Sagittal
TR (ms)	2,500–3,000	4,200	3,000	3,130	2,500–3,000	4,220
TE (ms)	103	98	101	101	103	100
Field of view (mm)	200×200	200×200	200×200	200×200	180×180	180×180
Matrix	320×320	320×288	320×320	320×320	320×320	640×640
Flip angle (°)	136	120	148	148	136	114
Slice thickness (mm)	3	4	3	4	3	3
Gap	0	0	0	0	0	0
NEX	2	4	2	4	2	6

T2WI, T2-weighted imaging; TR, repetition time; TE, echo time; NEX, number of excitations.

US Examination

Transrectal US biopsy was performed by one of four board-certified radiologists with 5, 6, 10, or 22 years of experience in prostate US, using a Philips iU22, Philips EPIQ 7 (Philips Medical Systems, Bothell, WA, USA) or a GE LOGIQ E10 (GE Healthcare, Milwaukee, WI, USA) device. The radiologists routinely obtained multiple axial and sagittal images of the prostate gland before biopsy.

Prostate Gland Volume Estimation Based on the Ellipsoid Formula

Two radiologists with 6 or 11 years of experience in prostate imaging independently measured the prostate gland diameters on the images obtained using both imaging modalities: AP diameter and transverse diameter on axial images and AP diameter and longitudinal diameter on midsagittal images (Fig. 2). Each radiologist retrospectively reviewed T2WI MRI and US images and measured the diameters on the picture archiving and communication system. In axial images, the radiologists found the plane depicting the maximal transverse diameter and measured the transverse and AP diameters on that plane [19]. The AP diameter was measured between the anterior and posterior margin of the prostate capsule, excluding the periprostatic vein. The longitudinal diameter was measured on the midsagittal plane that best showed the prostatic urethra. The longitudinal diameter is usually measured from the bladder neck to the prostate apex [20]. However, measurements of the longitudinal diameter can vary because of multiple landmarks. In this study, the superior margin was the bladder base, defined as a line connecting the anterior and posterior points where the bladder wall connected with prostate gland [21]. If the prostate tissue protruded above the line on the midsagittal plane, the proximal margin of the prostate tissue was used as the superior margin. The inferior landmark was the caudal margin of the peripheral zone defining the apex. As it is difficult to determine due to urethral continuation, an interpolated line connecting the margin of the peripheral zone located anterior and posterior to the urethra was used [21]. If there was prostate cancer with bulging contours or extensive prostate cancer replacing the prostate gland itself, the entire tumor was included in the prostate volume and diameter measurements.

Using the ellipsoid formula (prostate gland volume=AP diameter×transverse diameter×longitudinal diameter×0.52),

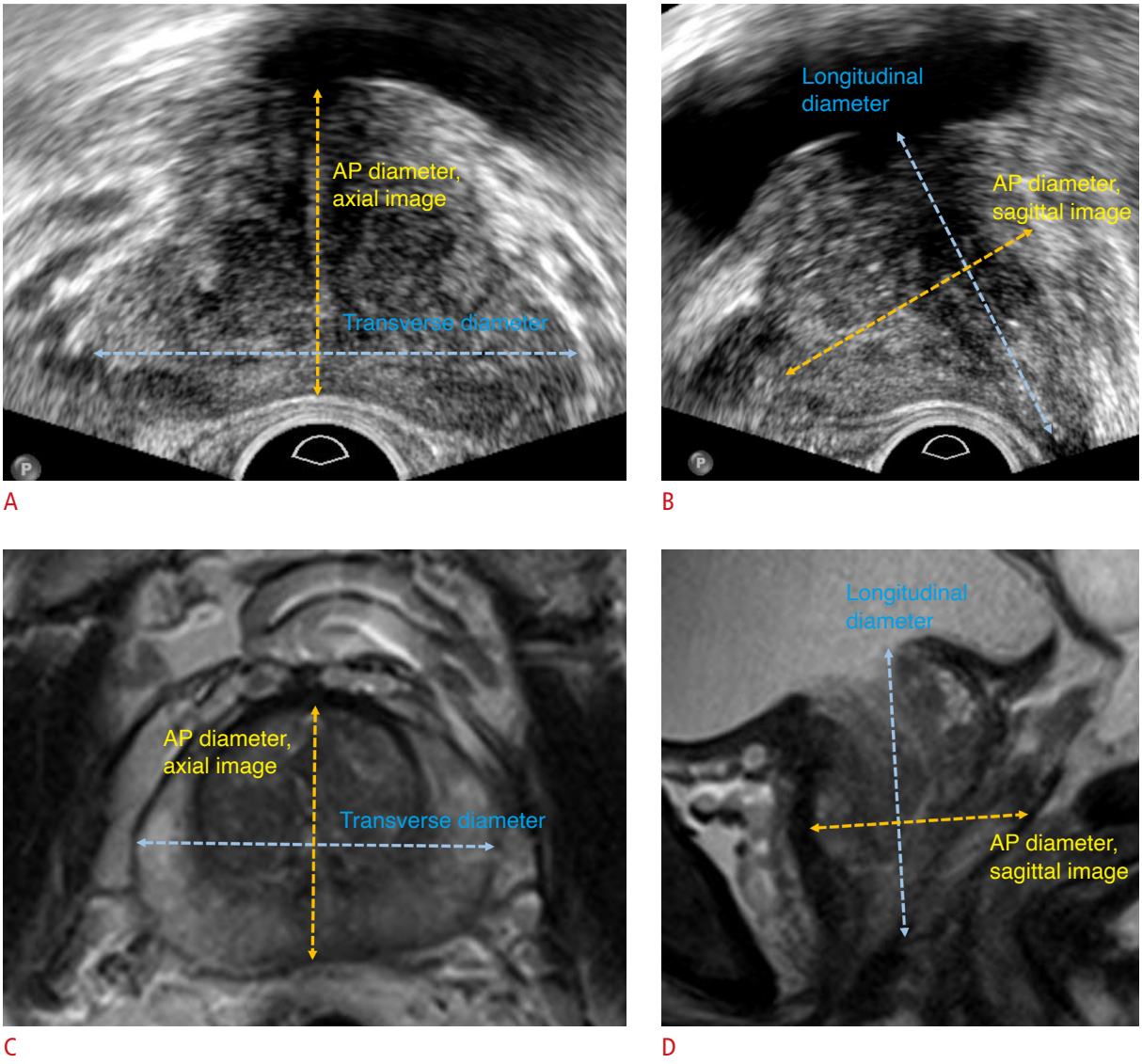

Fig. 2. Measurements using ellipsoid formulas ($volume_{ax}$ and $volume_{sag}$) when calculating prostate volume on ultrasonography (US) and magnetic resonance imaging (MRI).
A. The maximum transverse diameter and anteroposterior (AP) diameter were measured on axial US image. B. The maximum longitudinal diameter and AP diameter were measured on midsagittal US image. C. The maximum transverse diameter and AP diameter were measured on axial T2-weighted imaging (T2WI) of MRI. D. Maximum longitudinal diameter and AP diameter were measured on midsagittal T2WI of MRI.

$volume_{ax}$ (using the AP diameter from axial images) and $volume_{sag}$ (using the AP diameter from sagittal images) figures were calculated from US and MRI, respectively, to obtain US $volume_{ax}$, US $volume_{sag}$, MRI $volume_{ax}$ and MRI $volume_{sag}$. The transverse diameter and longitudinal diameter were commonly used on each examination to calculate the volume.

Prostate Gland Segmentation on MRI and Gold Standard Prostate Gland Volume

Segmentation of the prostate gland was carried out in three steps. First, prostate gland segmentation was performed using noncommercially available, deep learning-based prototype software (Prostate AI version 1.2.4, Siemens Healthcare). The algorithm was trained and validated with 2,170 biparametric MRI scans [22] and included the function of prostate segmentation, lesion detection, and PIRADS classification of the lesions [23]. Only the automatic gland segmentation function was used in this study. Whole-gland segmentation is performed on the T2WI volume using a deep learning-based convolutional neural network, and the prostate gland volume was measured based on the segmentation [24]. The

details of artificial intelligence algorithm are summarized in the Supplementary Material. Second, each case was randomly assigned to one of the two radiologists who had measured the prostate gland diameters, who then reviewed the MRI segmentation results. If needed, the radiologists manually revised the segmentation using a correction tool in the prototype software. If there was prostate cancer with bulging contours or extensive prostate cancer replacing the prostate gland, the entire tumor was included in the segmentation. Finally, a third radiologist, who did not participate in either measuring the prostate gland diameters or revising the prostate segmentation, confirmed that the final segmentation after the manual revision was correct. The prostate gland volume extracted from the segmentation was called the segmented volume and was considered to be the gold standard.

Statistical Analysis

Before the specific analysis, the normality of the data distribution was evaluated by the Kolmogorov–Smirnov test. All variables, including the diameters and prostate volume estimates, were non-normally distributed (P<0.001). Next, the differences in the two radiologists' measurements were analyzed. The differences in the four types of diameters and two types of volume estimates, as measured by the two radiologists, were compared using Wilcoxon signed-rank test on US and MRI. Inter-reader agreement between the two radiologists for each measurement was assessed by using a two-way random intraclass correlation coefficient (ICC). The ICC was interpreted as follows: <0.5, poor; 0.5–0.75, moderate; 0.75–0.9, good; and >0.9, excellent agreement. Inter-reader agreement was assessed using Bland-Altman plots.

Next, inter-method agreement between the $volume_{ax}$ and $volume_{sag}$ was analyzed using ICC and Bland-Altman plots on US and MRI, respectively. The AP diameters on axial and sagittal images, as well as $volume_{ax}$ and $volume_{sag}$ were compared using the Wilcoxon signed-rank test for US and MRI. Lastly, the four types of volume estimates by ellipsoid methods were compared with segmented volume (i.e., the gold standard) using the Wilcoxon signed-rank test and Bland-Altman plots. Agreement between the gold standard and the volume estimates was assessed by using ICCs. The volume difference was calculated for the four types of volume estimates as follows: segmented volume minus estimated volume. The correlations between the volume difference and segmented volume were evaluated using the Pearson correlation test (r) and displayed on scatter plots.

Statistical analysis was performed using SPSS software version 24.0 (IBM Corp., Armonk, NY, USA) and GraphPad Prism version 8.0 (GraphPad Software, Inc., La Jolla, CA, USA). A P-value <0.05 was considered statistically significant.

Results

The baseline characteristics of the 456 patients are summarized in Table 2. The mean age of the patients was 68.9 years (standard deviation, ±8.4 years). The median interval between MRI and US was 19 days.

The diameters and volumes measured by the two radiologists and ICCs between the two radiologists are presented in Table 3. While the AP diameters measured on axial MRI, as well as those on sagittal MRI, were not significantly different between the two radiologists, the other types of diameters showed significant differences. All measurements showed excellent inter-reader agreement (ICC >0.9). Supplementary Fig. 1 shows that, as the average prostate gland volume increased, the difference between the two radiologists' measurements tended to increase. The 95% limits of agreement between the two radiologists for the four volume estimates appeared similar.

The inter-method agreement between measurements on axial and sagittal images is shown in Table 4. Both reviewers' results commonly showed excellent inter-method agreement in all measurements, except for AP diameters on US, which showed good agreement. As shown in Supplementary Fig. 2, the 95% limits of agreement between $volume_{ax}$ and $volume_{sag}$ were slightly wider on US than on MRI, and there was no systematic bias between the two methods.

The median segmented prostate volume was 37.00 mL. Despite the significant differences between the volume estimates

Table 2. Baseline characteristics of the included patients (n=456)

Characteristic	Value
Age (year)	68.9±8.4
PSA (ng/mL)	7.8 (5.0–16.0)
Interval between MRI and ultrasound (day)	19 (7–34)
Pathologically proven prostate cancer	277 (60.7)
Pathologically proven CSC	251 (55.0)
Radical prostatectomy	163 (35.7)
Interval between MRI and prostatectomy (day)	67.0 (44.8–92.0)
Gleason grade (n=277)	
1	31 (11.1)
2	103 (37.2)
3	68 (24.5)
4	47 (17.0)
5	28 (17.0)

Values are presented as mean±SD, median (IQR), and number (%).
PSA, prostate-specific antigen; MRI, magnetic resonance imaging; CSC, clinically significant prostate cancer; SD, standard deviation; IQR, interquartile range.

Table 3. Differences and intraclass correlation coefficients in parameters measured by two radiologists

	Radiologist 1	Radiologist 2	P-value[a)]	ICC
MRI				
AP diameter, axial image (cm)	3.60 (3.10–4.00)	3.55 (3.10–4.00)	0.207	0.950
AP diameter, sagittal image (cm)	3.60 (3.20 –4.10)	3.60 (3.20–4.10)	0.789	0.948
Transverse diameter (cm)	4.90 (4.50–5.40)	5.00 (4.60–5.50)	<0.001	0.945
Longitudinal diameter (cm)	4.20 (3.90–4.80)	4.40 (4.00–4.90)	<0.001	0.942
$Volume_{ax}$ (mL)	38.10 (29.46–51.97)	40.67 (30.83–54.82)	<0.001	0.975
$Volume_{sag}$ (mL)	39.87 (30.12–53.44)	41.27 (31.74–56.04)	<0.001	0.975
Ultrasonography				
AP diameter, axial image (cm)	3.30 (2.80–3.80)	3.20 (2.80–3.70)	<0.001	0.953
AP diameter, sagittal image (cm)	3.40 (3.00–3.80)	3.40 (3.00–3.80)	0.018	0.926
Transverse diameter (cm)	5.00 (4.60–5.30)	5.00 (4.60–5.40)	<0.001	0.925
Longitudinal diameter (cm)	4.20 (3.80–4.80)	4.10 (3.70–4.70)	<0.001	0.933
$Volume_{ax}$ (mL)	37.79 (26.21–48.41)	34.30 (25.41–46.76)	<0.001	0.974
$Volume_{sag}$ (mL)	36.69 (28.23–49.03)	36.54 (27.09–47.93)	0.008	0.960

Values are presented as median (interquartile range).
ICC, intraclass correlation coefficient; MRI, magnetic resonance imaging; AP, anteroposterior.
$Volume_{ax}$=AP diameter on axial image×transverse diameter×longitudinal diameter×0.52; $Volume_{sag}$=AP diameter on sagittal image×transverse diameter×longitudinal diameter×0.52.
[a)]The results of the Wilcoxon signed-rank test.

Table 4. Inter-method agreement in two types of AP diameters on axial and sagittal images, and two types of prostate gland volume estimates ($volume_{ax}$ and $volume_{sag}$)

	Radiologist 1		Radiologist 2	
	P-value[a)]	ICC	P-value[a)]	ICC
MRI				
AP diameter, axial image vs. sagittal image	<0.001	0.950	<0.001	0.935
$Volume_{ax}$ vs. $volume_{sag}$	<0.001	0.992	<0.001	0.990
Ultrasonography				
AP diameter, axial image vs. sagittal image	<0.001	0.887	<0.001	0.890
$Volume_{ax}$ vs. $volume_{sag}$	<0.001	0.977	<0.001	0.982

AP, anteroposterior; ICC, intraclass correlation coefficient; MRI, magnetic resonance imaging.
$Volume_{ax}$=AP diameter on axial image×transverse diameter×longitudinal diameter×0.52; $Volume_{sag}$=AP diameter on sagittal image×transverse diameter×longitudinal diameter×0.52.
[a)]The results of the Wilcoxon signed-rank test.

and segmented volume, all volume estimates showed excellent agreement with the gold standard (ICC >0.9) (Table 5). The median MRI volume was larger than the segmented volume, and the US volume was smaller than the segmented volume. In Fig. 3, the volume estimates on US showed a slightly wider 95% limit of agreement than MRI.

The volume difference between the volume estimates and segmented volume increased as the prostate gland volume increased in all four types of estimates (P<0.001), with greater difference on US than on MRI in patients with larger prostate glands (Fig. 4).

Discussion

This study compared the prostate volume estimates using two different AP diameters measured on axial and sagittal images by US and MRI in a large number of patients (n=456). The four types of volume estimates from the ellipsoid formula on US and MRI were compared to the gold standard (segmented volume) that was extracted from the segmented masks of the entire prostate gland on MRI. On both US and MRI, the difference between $volume_{ax}$ and $volume_{sag}$ was small in absolute values but statistically significant.

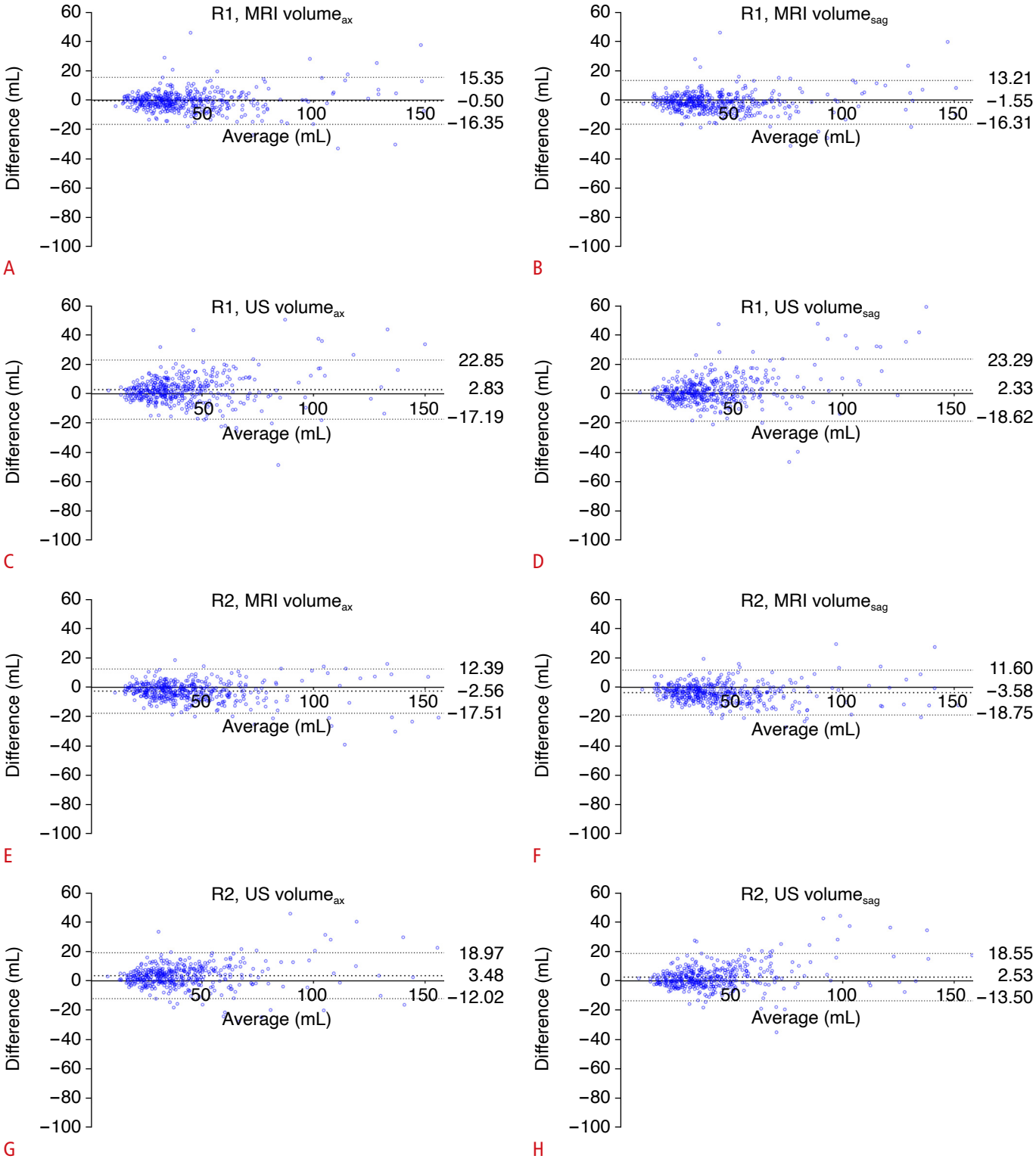

Fig. 3. Differences between the volume estimates and segmented volume.
Bland-Altman plots show the differences between the segmented volume and volume estimates measured by two radiologists. The results for radiologist 1 for magnetic resonance imaging (MRI) volume$_{ax}$, MRI volume$_{sag}$, ultrasonography (US) volume$_{ax}$, and US volume$_{sag}$ are shown in A, B, C, and D, respectively, and the results for radiologist 2 are shown in the same order in E, F, G, and H, respectively. The thick dotted lines indicate mean differences, and the thin dotted lines indicate 95% limits of agreement. Average, the average of the segmented volume and volume estimates; Difference, segmented−volume estimates; R1, radiologist 1; R2, radiologist 2; volume$_{ax}$=AP diameter on axial image×transverse diameter×longitudinal diameter×0.52; volume$_{sag}$=AP diameter on sagittal image×transverse diameter×longitudinal diameter×0.52.

Even though all volume estimates showed excellent correlations with the gold standard prostate volume, the volume estimates were significantly different from the gold standard. The results of this study suggest that the prostate AP diameter should be consistently measured on either the axial or sagittal plane and on either US or MRI to generate consistent volume estimations.

On MRI, measuring the AP diameter on axial images and on sagittal images follows the PIRADS version 2.0 and version 2.1 recommendations, respectively. PIRADS version 2.1 changed the plane used to measure the AP diameter from axial to sagittal, because axial MRI images are not necessarily parallel to the short axis of the prostate gland. A previous study showed that using the ellipsoid formula for the AP diameter on axial images (PIRADS version 2.0 recommendation) yielded the most accurate volume estimates [18]. The present study also showed similar results: MRI $volume_{ax}$ showed a more similar median value to the segmented volume than MRI $volume_{sag}$. Therefore, the ellipsoid formula using the AP diameter on axial images may also lead to sufficiently accurate estimations of the prostate gland volume.

We applied the same concept of volume measurement as with MRI to US and obtained different results. The median US $volume_{ax}$ was much smaller than the segmented volume, compared with the US $volume_{sag}$, even though the volume estimates on US showed excellent agreement with the segmented volume. Based on the results of the present study, the AP diameters on sagittal US images and those on axial MRI images are preferable to estimate prostate gland volume, and these results are similar to the findings of a previous study [9]. However, there is another study that showed different results: the US $volume_{ax}$ was not significantly different from the US $volume_{sag}$, but the US $volume_{ax}$ was better correlated with the volume measured after prostatectomy [25].

Like previous studies, the MRI-based ellipsoid formula overestimated, and the US-based method underestimated prostate gland volume in the current study [26,27]. The AP diameter of the prostate may decrease due to compression by the ultrasound probe during the examination, and the volume may be underestimated [28]. PSAD calculated with a US-based volume estimate likely overstates the risk of prostate cancer compared with that calculated using an MRI-based volume estimate. Additionally, the volume difference (segmented volume−volume estimate) was significantly correlated with prostate gland volume. The four kinds of volume estimates all showed greater differences in patients with large prostate gland volumes, especially on US. These results mean that the imaging

Table 5. Differences and agreement between the gold standard (segmented volume) and the volume estimated by the ellipsoid formula

	Value	P-value[a)]	ICC
Segmented volume	37.00 (28.33–51.53)	–	–
Radiologist 1			
MRI $volume_{ax}$ (mL)	38.10 (29.46–51.97)	0.001	0.970
MRI $volume_{sag}$ (mL)	39.87 (30.12–53.44)	<0.001	0.974
US $volume_{ax}$ (mL)	34.79 (26.21–48.41)	<0.001	0.942
US $volume_{sag}$ (mL)	36.69 (28.23–49.03)	<0.001	0.930
Radiologist 2			
MRI $volume_{ax}$ (mL)	40.66 (30.83–54.82)	<0.001	0.975
MRI $volume_{sag}$ (mL)	41.27 (31.74–56.04)	<0.001	0.973
US $volume_{ax}$ (mL)	34.30 (25.41–46.76)	<0.001	0.967
US $volume_{sag}$ (mL)	36.54 (27.09–47.93)	<0.001	0.963

ICC, intraclass correlation coefficient; MRI, magnetic resonance imaging; US, ultrasonography.
[a)]The results of the Wilcoxon signed-rank test.

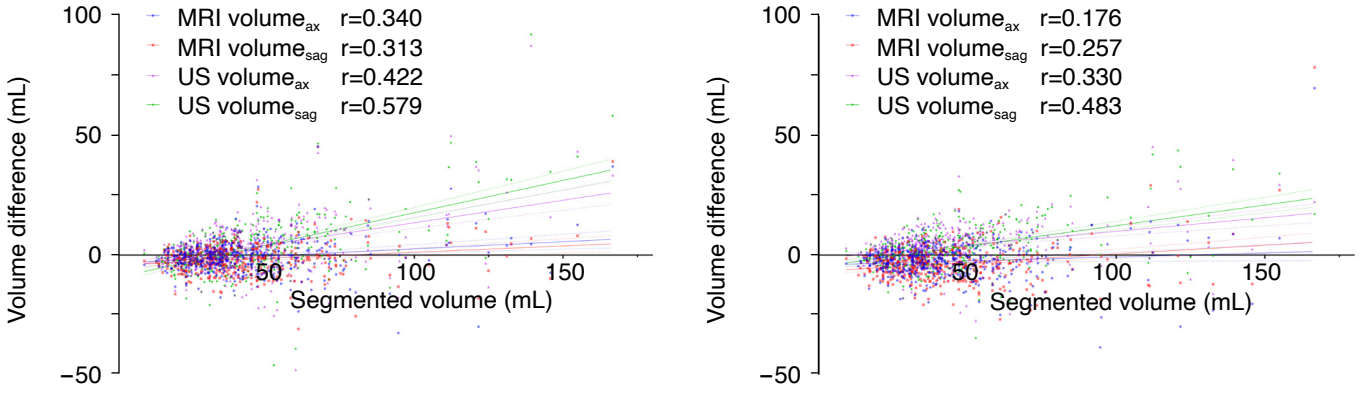

A B

Fig. 4. Scatter plots depicting the relationship of the segmented volume with volume difference.
The segmented volume of the prostate gland and volume difference (segmented volume−volume estimate) for all methods show positive correlations for radiologist 1 (A) and radiologist 2 (B). MRI, magnetic resonance imaging; US, ultrasonography.

tended to underestimate the larger prostate glands, as a previous study showed [26]. The correlation coefficient between the volume difference and segmented volume was higher for US than for MRI. These results imply more accurate volume estimation on MRI than US, similar to that reported in a systematic review [26]. These results may be due to the relatively small field of view in US, which may not include the entire prostate gland if it has a large volume.

The inter-method agreement between $volume_{ax}$ and $volume_{sag}$ was excellent (ICC >0.9) for both MRI and US by both radiologists. However, the 95% limits of agreement in Bland-Altman plots between the two methods were wider for US than for MRI. The differences between the two methods tended to increase as the prostate gland volume increased. In some patients with large prostate glands (>100 mL), the difference between the volume estimates using the two methods was approximately 20 mL, which was considerable. Therefore, consistently using axial or sagittal images to measure the AP diameter seems important in daily practice to eliminate the inaccuracy in volume estimation by the two methods.

The AP diameters on axial and sagittal images between the two radiologists were similar for MRI but significantly different for US. Interestingly, significant differences were observed in the transverse and longitudinal diameters between the two radiologists on both US and MRI. Nevertheless, all measurements for both US and MRI showed excellent inter-reader agreement (ICC >0.9), and no systematic bias was found on Bland-Altman plots. Therefore, the selection of either axial or sagittal images for measuring AP diameter appears to not be very important in terms of maintaining high inter-reader agreement between US and MRI. Instead, more precise guidelines to measure transverse and longitudinal diameters may be necessary.

Some limitations of this study should be noted. First, this study used transrectal US images that had already been obtained during clinical practice. To minimize the variability in image quality that may be caused by physician experience, only patients who underwent prostate US performed by board-certified radiologists were included. Second, the gold standard of prostate volume was extracted from whole-gland segmentation on MRI rather than a volume measurement of pathologic specimens. However, the ellipsoid formula was unable to reflect the real shape of the prostate gland, even for prostatectomy specimens [27]. Estimating the prostate gland volume by converting the prostate weight using tissue density also has the potential to be inaccurate [9]. Third, extensive prostate cancer was included in the prostate segmentation. Given that cancer is not differentiated from the normal prostate gland when measuring prostate gland volume in routine practice, including prostate cancer in the prostate gland appeared to be a more practical way to measure prostate gland volume.

In conclusion, $volume_{ax}$ and $volume_{sag}$ showed excellent inter-method agreement and excellent agreement with the gold standard on both US and MRI. However, the prostate volume was overestimated on MRI and underestimated on US.

ORCID: Seo Yeon Youn: https://orcid.org/0000-0002-7692-3413; Moon Hyung Choi: https://orcid.org/0000-0001-5962-4772; Young Joon Lee: https://orcid.org/0000-0001-8309-0272; Robert Grimm: https://orcid.org/0000-0002-1233-8215; Heinrich von Busch: https://orcid.org/0000-0003-0469-1622; Dongyeob Han: https://orcid.org/0000-0002-1402-5036; Yohan Son: https://orcid.org/0000-0002-6075-2090; Bin Lou: https://orcid.org/0000-0002-4687-8519; Ali Kamen: https://orcid.org/0000-0002-1928-2410

Author Contributions

Conceptualization: Choi MH, Lee YJ. Data acquisition: Youn SY, Choi MH. Data analysis or interpretation: Youn SY, Choi MH, Grimm R, von Busch H, Han D, Son Y, Lou B, Kamen A. Drafting of the manuscript: Youn SY, Choi MH. Critical revision of the manuscript: Youn SY, Choi MH, Lee YJ, Grimm R, von Busch H, Han D, Son Y, Lou B, Kamen A. Approval of the final version of the manuscript: all authors.

Conflict of Interest

Moon Hyung Choi is currently receiving a research grant from Siemens Healthineers for a topic not related to the current research. Robert Grimm, Heinrich von Busch, Dongyeob Han, Yohan Son, Bin Lou, and Ali Kamen are employees of Siemens Healthineers/Healthcare. For the remaining authors, no conflicts of interest are declared. This research did not receive any specific grant from funding agencies in the public, commercial, or not-for-profit sectors.

Supplementary Material

Supplementary Material. Details of artificial intelligence algorithm to segment prostate gland on MRI. The segmentation model takes the entire 3D radiological volume as input, and outputs the probability maps that indicate how likely voxels belongs to the target region or interest. A deep dense fully convolutional encoder-decoder neural network was adopted. It has an overall v-net architecture with dense blocks. Each dense block has a batchnorm, convolution/deconvolution, leaky ReLU repeated with dense connections. The v-net part allows for higher resolution by concatenating features from the downsampling part to the upsampling part of the network (skip connections). Training was done using AdaBound optimizer with constant learning rate of 0.001 and Jaccard Index as the loss function. (https://doi.org/10.14366/usg.22104).

Supplementary Fig. 1. Interreader agreement in prostate gland volume estimates measured by two radiologists. Bland atlman plots show the differences in the prostate gland volume calculated

using anteroposterior (AP) diameter on axial MRI (A), sagittal MRI (B), axial ultrasonography (US) (C) and sagittal US (D) images. The thick dot lines indicate mean differences and thin dot line indicate 95% limits of agreement. Average, the average of the two measurements; difference, volume measured by reviewer 1-that by reviewer 2; $volume_{ax}$=AP diameter on axial image×transverse diameter×longitudinal diameter×0.52; $volume_{sag}$=AP diameter on sagittal image×transverse diameter×longitudinal diameter×0.52. (https://doi.org/10.14366/usg.22104).

Supplementary Fig. 2. The difference in prostate gland volume estimates according to the different anteroposterior (AP) diameters. Bland Altman plots show the differences in $volume_{sag}$ and $volume_{ax}$ on MRI and ultrasonography (US) by reviewer 1 (A, B) and reviewer 2 (C, D), respectively. The thick dot lines indicate mean differences and thin dot line indicate 95% limits of agreement. Average, the average of the $volume_{ax}$ and $volume_{sag}$; Difference, $volume_{ax}$–$volume_{sag}$; $volume_{ax}$=AP diameter on axial image×transverse diameter×longitudinal diameter×0.52; $volume_{sag}$=AP diameter on sagittal image×transverse diameter×longitudinal diameter×0.52. (https://doi.org/10.14366/usg.22104).

References

1. McVary KT, Kaplan SA. A Tower of babel in today's urology: disagreement in concepts and definitions of lower urinary tract symptoms/benign prostatic hyperplasia re-treatment. J Urol 2020;204:213-214.
2. Wei JT, Calhoun E, Jacobsen SJ. Urologic diseases in America project: benign prostatic hyperplasia. J Urol 2005;173:1256-1261.
3. Egan KB. The Epidemiology of benign prostatic hyperplasia associated with lower urinary tract symptoms: prevalence and incident rates. Urol Clin North Am 2016;43:289-297.
4. Sung H, Ferlay J, Siegel RL, Laversanne M, Soerjomataram I, Jemal A, et al. Global cancer statistics 2020: GLOBOCAN estimates of incidence and mortality worldwide for 36 cancers in 185 countries. CA Cancer J Clin 2021;71:209-249.
5. Tewari A, Indudhara R, Shinohara K, Schalow E, Woods M, Lee R, et al. Comparison of transrectal ultrasound prostatic volume estimation with magnetic resonance imaging volume estimation and surgical specimen weight in patients with benign prostatic hyperplasia. J Clin Ultrasound 1996;24:169-174.
6. Lee SJ, Oh YT, Jung DC, Cho NH, Choi YD, Park SY. Combined analysis of biparametric MRI and prostate-specific antigen density: role in the prebiopsy diagnosis of Gleason score 7 or greater prostate cancer. AJR Am J Roentgenol 2018;211:W166-W172.
7. Magheli A, Rais-Bahrami S, Trock BJ, Humphreys EB, Partin AW, Han M, et al. Prostate specific antigen versus prostate specific antigen density as a prognosticator of pathological characteristics and biochemical recurrence following radical prostatectomy. J Urol 2008;179:1780-1784.
8. Radwan MH, Yan Y, Luly JR, Figenshau RS, Brandes SB, Bhayani SB, et al. Prostate-specific antigen density predicts adverse pathology and increased risk of biochemical failure. Urology 2007;69:1121-1127.
9. Jeong CW, Park HK, Hong SK, Byun SS, Lee HJ, Lee SE. Comparison of prostate volume measured by transrectal ultrasonography and MRI with the actual prostate volume measured after radical prostatectomy. Urol Int 2008;81:179-185.
10. Matthews GJ, Motta J, Fracehia JA. The accuracy of transrectal ultrasound prostate volume estimation: clinical correlations. J Clin Ultrasound 1996;24:501-505.
11. Ahmed HU, El-Shater Bosaily A, Brown LC, Gabe R, Kaplan R, Parmar MK, et al. Diagnostic accuracy of multi-parametric MRI and TRUS biopsy in prostate cancer (PROMIS): a paired validating confirmatory study. Lancet 2017;389:815-822.
12. Elwenspoek MM, Sheppard AL, McInnes MD, Merriel SW, Rowe EW, Bryant RJ, et al. Comparison of multiparametric magnetic resonance imaging and targeted biopsy with systematic biopsy alone for the diagnosis of prostate cancer: a systematic review and meta-analysis. JAMA Netw Open 2019;2:e198427.
13. van der Leest M, Cornel E, Israel B, Hendriks R, Padhani AR, Hoogenboom M, et al. Head-to-head comparison of transrectal ultrasound-guided prostate biopsy versus multiparametric prostate resonance imaging with subsequent magnetic resonance-guided biopsy in biopsy-naive men with elevated prostate-specific antigen: a large prospective multicenter clinical study. Eur Urol 2019;75:570-578.
14. Kasivisvanathan V, Rannikko AS, Borghi M, Panebianco V, Mynderse LA, Vaarala MH, et al. MRI-targeted or standard biopsy for prostate-cancer diagnosis. N Engl J Med 2018;378:1767-1777.
15. Turkbey B, Rosenkrantz AB, Haider MA, Padhani AR, Villeirs G, Macura KJ, et al. Prostate imaging reporting and data system version 2.1: 2019 update of prostate imaging reporting and data system version 2. Eur Urol 2019;76:340-351.
16. Weinreb JC, Barentsz JO, Choyke PL, Cornud F, Haider MA, Macura KJ, et al. PI-RADS prostate imaging - reporting and data system: 2015, version 2. Eur Urol 2016;69:16-40.
17. An JY, Fowler KJ. Accurate prostate volumes from manual calculations: a comparison of PI-RADS v2 and v2.1 measurement techniques. Acad Radiol 2021;28:1557-1558.
18. Ghafoor S, Becker AS, Woo S, Causa Andrieu PI, Stocker D, Gangai N, et al. Comparison of PI-RADS versions 2.0 and 2.1 for MRI-based calculation of the prostate volume. Acad Radiol 2021;28:1548-1556.
19. Choi YJ, Kim JK, Kim HJ, Cho KS. Interobserver variability of

transrectal ultrasound for prostate volume measurement according to volume and observer experience. AJR Am J Roentgenol 2009;192:444-449.
20. Littrup PJ, Williams CR, Egglin TK, Kane RA. Determination of prostate volume with transrectal US for cancer screening. Part II. Accuracy of in vitro and in vivo techniques. Radiology 1991;179:49-53.
21. Wasserman NF, Niendorf E, Spilseth B. Measurement of prostate volume with MRI (a guide for the perplexed): biproximate method with analysis of precision and accuracy. Sci Rep 2020;10:575.
22. Yu X, Lou B, Shi B, Winkel D, Arrahmane N, Diallo M, et al. False positive reduction using multiscale contextual features for prostate cancer detection in multi-parametric MRI scans. In: 2020 IEEE 17th International Symposium on Biomedical Imaging (ISBI); 2020 Apr 3-7; Iowa City, IA, USA. New York: Institute of Electrical and Electronics Engineers, 2020.
23. Winkel DJ, Tong A, Lou B, Kamen A, Comaniciu D, Disselhorst JA, et al. A novel deep learning based computer-aided diagnosis system improves the accuracy and efficiency of radiologists in reading biparametric magnetic resonance images of the prostate: results of a multireader, multicase study. Invest Radiol 2021;56:605-613.
24. Yang D, Xu D, Zhou SK, Georgescu B, Chen M, Grbic S, et al. Automatic liver segmentation using an adversarial image-to-image network. In: Medical Image Computing and Computed Assisted Intervention - MICCAI 2017; 2017 Sep 11-13; Quebec City, Canada. Cham: Springer, 2017;507-515.
25. Park SB, Kim JK, Choi SH, Noh HN, Ji EK, Cho KS. Prostate volume measurement by TRUS using heights obtained by transaxial and midsagittal scanning: comparison with specimen volume following radical prostatectomy. Korean J Radiol 2000;1:110-113.
26. Christie DR, Sharpley CF. How accurately can prostate gland imaging measure the prostate gland volume? Results of a systematic review. Prostate Cancer 2019;2019:6932572.
27. Massanova M, Robertson S, Barone B, Dutto L, Caputo VF, Bhatt JR, et al. The comparison of imaging and clinical methods to estimate prostate volume: a single-centre retrospective study. Urol Int 2021;105:804-810.
28. Roehrborn CG, Girman CJ, Rhodes T, Hanson KA, Collins GN, Sech SM, et al. Correlation between prostate size estimated by digital rectal examination and measured by transrectal ultrasound. Urology 1997;49:548-557.